Perpendicular magnetic anisotropy in chemically disordered FePd–FeV(100) alloy thin films

C. Clavero,[a] J. M. García-Martín, G. Armelles, and A. Cebollada
Instituto de Microelectrónica de Madrid-IMM (CNM-CSIC), Isaac Newton 8-PTM, E-28760 Tres Cantos, Madrid, Spain

Y. Huttel
Instituto de Ciencia de Materiales de Madrid (ICMM-CSIC), E-28049 Cantoblanco, Madrid, Spain

S. Estradé, J. Arbiol, and F. Peiró
EME Electronic Materials and Engineering, Department Electronics, University of Barcelona, Martí i Franquès 1, E-08028 Barcelona, Spain

Ll. Balcells
Instituto de Ciencia de Materiales de Barcelona-ICMAB (CSIC), Campus de la Universidad Autònoma de Barcelona, E-08193 Bellaterra, Spain

(Received 3 October 2005; accepted 9 February 2006; published online 10 April 2006)

We find that the use of V(100) buffer layers on MgO(001) substrates for the epitaxy of FePd binary alloys yields to the formation at intermediate and high deposition temperatures of a FePd–FeV mixed phase due to strong V diffusion accompanied by a loss of layer continuity and strong increase of its mosaic spread. Contrary to what is usually found in this kind of systems, these mixed phase structures exhibit perpendicular magnetic anisotropy (PMA) which is not correlated with the presence of chemical order, almost totally absent in all the fabricated structures, even at deposition temperatures where it is usually obtained with other buffer layers. Thus the observed PMA can be ascribed to the V interdiffusion and the formation of a FeV alloy, being the global sample saturation magnetization also reduced. © *2006 American Institute of Physics*. [DOI: 10.1063/1.2187413]

I. INTRODUCTION

The fabrication of binary FePt and FePd alloys is of great fundamental and technological interests. These alloys in their chemically ordered phase ($L1_0$) exhibit large perpendicular magnetic anisotropy (PMA): $K_u \sim 10^7$ J/m^3 in FePt and $K_u \sim 9\times10^5$ J/m^3 in FePd.[1] Chemical order is characterized by the alternation of pure Fe and Pd (Pt) atomic planes along a cubic (001) direction, which as a consequence suffers a tetragonal distortion with respect to the cubic lattice, and becomes the axis for easy magnetization. Therefore, chemically ordered $L1_0$ films grown along the (001) direction exhibit PMA. On the other hand, in magnetic nanoparticle systems the thermal stability of the magnetization in individual nanoparticles scales with the anisotropy constant (K_u) and the nanoparticle volume;[2] therefore with the presence of such a high magnetic anisotropy phase it is possible to reduce strongly the nanoparticle size while avoiding the so called superparamagnetic limit. These features make them excellent candidates to develop ultrahigh density magnetic media with naturally separated and stable bits.[3,4] The onset of chemical order and therefore large magnetic anisotropy in FePd and FePt binary alloys is associated with the chemical order degree, only being achieved at high enough deposition or annealing temperatures [400 °C for FePd (Ref. 5) and 600 °C for FePt (Ref. 6)], a fact that can be a drawback for the production of technological devices. In this scope alternative methods used in recent years to obtain PMA in alloys grown at a lower temperature and with a smaller chemical ordering degree include the addition of third elements,[7] artificial multilayering,[8] ion irradiation,[9] monoatomic layer control,[10] compositional changes,[11] and selection of buffer layer nature.[12]

This last method, a buffer layer between the substrate and the binary alloy, is generally used to increase the flatness of the initial growing surface and to decrease the existent lattice mismatch, and it has been demonstrated that the nature,[5,10–17] thickness,[5] and deposition temperature[13] of the buffer layer affect strongly the ordering degree of the binary alloy. Amongst a large variety of materials, V has never been used as a buffer layer for the epitaxy of FePt and FePd alloys, in spite of the high flatness and crystalline quality of V(100) thin films grown on MgO(001) substrates[18] with interfacial roughness between 1 and 3 Å.

Therefore the motivation of this work is to study the structure, morphology, composition, magnetism, and magneto-optical (MO) response of FePd films sputter deposited at temperatures between room temperature (RT) and 700 °C on monocrystalline V(001) buffer layers grown on MgO(001) substrates. A PMA phase is obtained in FePd films grown at temperatures above 400 °C in spite of the fact that no chemical ordering is found. A strong V interdiffusion into the FePd layer and the formation of FeV alloy is accompanied by a two-dimensional to three-dimensional growth mode transition and an increase of the mosaic spread at these temperatures. Although in this case PMA is obtained at similar temperatures as in regular FePd alloys, in this approxima-

[a]Author to whom correspondence should be addressed; electronic mail: cesarcl@imm.cnm.csic.es

tion FePd–FeV mixed systems can open alternative ways to obtain high anisotropy systems at lower temperatures and with lower chemical order requirements. The paper will be structured as follows: in Sec. II the experimental details are reported. In Sec. III the evolution of the different structural aspects, such as morphology, crystalline structure, and interface nature, as a function of the alloy deposition temperature will be described. Then Sec. IV will show the effects that these structural aspects have in different magnetic and magneto-optical properties, such as saturation magnetization, magnetic anisotropy, and magneto-optical activity. Finally, Sec. V will be devoted to presenting the main conclusions of the work.

II. EXPERIMENT

FePd films of 22 nm in thickness were obtained by triode sputtering codeposition from Fe and Pd targets at 4×10^{-4} mbar Ar pressure in an ultrahigh-vacuum chamber with a base pressure in the low 10^{-9} mbar range. The alloys were grown at different deposition temperatures, ranging from RT up to 700 °C at a deposition rate of 0.24 Å/s. Prior to FePd deposition, a 40 Å buffer layer of V was deposited by sputtering at 400 °C on MgO(001) substrates at a deposition rate of 0.07 Å/s, optimum conditions for the growth of high crystalline quality, and low surface roughness epitaxial V films.[18] Subsequently to the FePd deposition, a 50 Å thick protective capping layer of Pd was deposited at RT also by sputtering.

A multitechnique approach has been followed to study the fabricated structures, using atomic force microscopy (AFM), x-ray diffraction (XRD), and transmission electron microscopy (TEM) for the structural characterization, electron energy loss spectroscopy (EELS), and x-ray photoemission spectroscopy (XPS) for the in-depth resolved chemical composition, and superconducting quantum interference device (SQUID), magnetic force microscopy (MFM), magneto-optical Kerr effect (MOKE) loops, and Kerr spectroscopy for the magnetic and MO characterizations. AFM and MFM images were taken using a Nanotec™ microscope operating in a noncontact dynamic mode. For MFM, the tip scanned at a constant lift height above the sample (typically 50 nm) and the phase shift, proportional to the force gradient, was measured. Probes with similar cantilevers (force constant ~5 N/m and resonant frequency ~150 kHz) and pyramidal tips (cone angle below 20°) but different magnetic coatings were used. All of them were magnetized along the pyramid axis. XRD and x-ray reflectometry (XRR) experiments were performed in a four-circle diffractometer with Cu $K\alpha$ ($\lambda = 1.5418$ Å) radiation, using Bragg-Brentano configuration and 1/4° slits. TEM characterization was carried out in a Jeol 2010 field emission gun microscope operating at 200 kV. In these measurements, EELS was also used to detect variation in the composition of different areas of the samples. EELS spectra were taken within a range of electron energy loss rating from 325 to 745 eV, in order to examine Pd $M_{4,5}$, V $L_{2,3}$, O K, and Fe $L_{2,3}$ peaks. XPS depth profiling was carried out to investigate the concentration and chemical states of the elements in the layers; the samples were etched using Ar^+ ions with 1 keV energy and the incidence angle of the impinging Ar^+ ions was 42° with respect to the normal of the sample. The angle between the hemispherical analyzer (Specs, PHOIBOS 100) and the normal of the surface was kept at 30°. The quantitative analysis was performed by the evolution of the photoemission integrated intensities of Fe $2p_{1/2}$, Fe $2p_{3/2}$, Pd $3d_{3/2}$, Pd $3d_{5/2}$, V $2p_{1/2}$, and V $2p_{3/2}$ transitions for each sample. Details on the determination of the Ar^+ etching rate can be found elsewhere.[19]

Magnetization measurements were carried out by using a rf-SQUID magnetometer from Quantum Design at RT in applied fields up to 20 kOe. The MO behavior of the samples was studied by means of transverse and polar MOKE loops. Transverse loops were measured with a 633 nm HeNe laser system at RT in 45° incidence angle geometry; the change in reflectance was registered; in the case of polar Kerr loops, 530 nm light in normal incidence also at RT was used and the Kerr rotation angle was measured. Moreover, polar Kerr spectra were measured in a spectrometer similar to the one described in Ref. 20, in the spectral range from 1.4 to 4.3 eV.

III. MORPHOLOGY AND STRUCTURE

AFM images were taken in all samples to investigate the surface morphology dependence on the alloy deposition temperature. Since the surface roughness of a 40 Å vanadium layer grown at 400 °C on MgO(001) is very low (with an interfacial roughness between 1 and 3 Å),[18] we can then expect all the observed features in the as grown structures to be in principle primarily due to the Pd capped FePd alloy thin films. In Figs. 1(a)–1(f) we show the results for six of the samples, representative of the three different morphology regimes obtained as a function of deposition temperature. In the case of the low deposition temperature regime, we show AFM images for the samples grown at RT and 300 °C [Figs. 1(a) and 1(b)]. At RT can be observed a very flat surface and only small circular shaped features with an average in-plane diameter of 50 nm and 0.5 nm height, of the same order of what is observed in the bare V buffer layers; while in the 300 °C sample [Fig. 1(b)] these features are larger with an average in-plane diameter of 150 nm and 1.9 nm height. Morphological changes become evident as the FePd deposition temperature is increased, observing a transition from two-dimensional to three-dimensional growth mode at 400 °C [Fig. 1(c)], where the film morphology is not continuous anymore and the sample surface exhibits cracks with features of 200 nm in width in average lateral dimensions and 17 nm in depth (the nominal thickness of the film being 22 nm). Above this temperature a clear three-dimensional growth mode is obtained, with the size of the nanoparticles continuously increasing with increasing deposition temperature. In Figs. 1(d)–1(f) we show AFM images for the samples grown at 500, 600, and 700 °C, respectively, representative of this growth mode regime, observing nanoparticles with mean diameters ranging from 600 to 750 nm and average height from 40 to 50 nm. In Fig. 1(g) AFM line scan profiles of samples grown at RT and 300, 400, 500, and

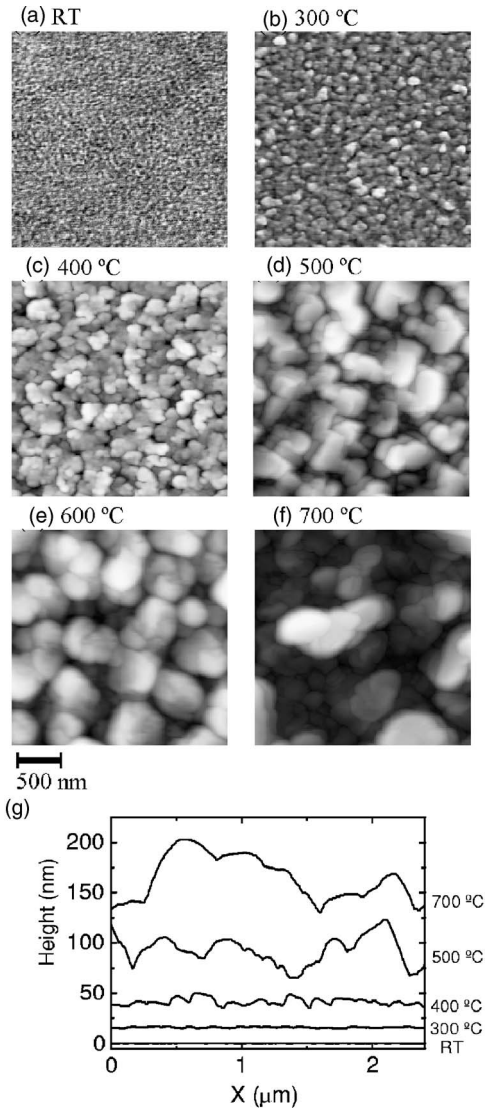

FIG. 1. AFM images corresponding to the samples grown at (a) RT and (b) 300, (c) 400, (d) 500, (e) 600, (f) and 700 °C. (g) Profiles of the samples grown at RT and 300, 400, 500, and 700 °C. A two-dimensional to three-dimensional growth mode transition is observed.

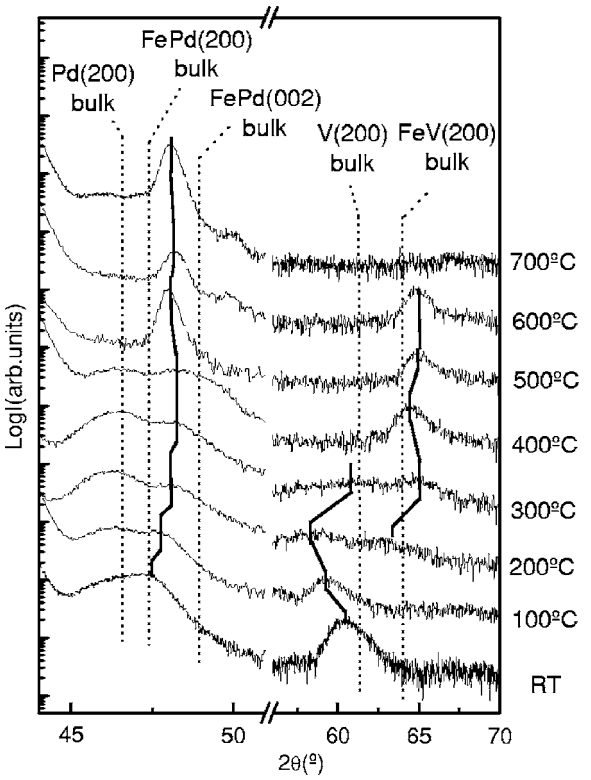

FIG. 2. Symmetric x-ray diffraction scans for the Pd/FePd/V/MgO structures with different FePd deposition temperatures. The position of Pd(200), FePd(200), FePd(002), V(200), and FeV(200) bulk peaks is indicated.

700 °C are presented, where the lateral and vertical dimensions of the surface features of the samples can be easily compared.

Complementary structural information, now focused on the alloy crystalline structure, was obtained by XRD. Symmetric and asymmetric XRD scans as well as rocking curves around the main reflections were measured for all the samples. In Fig. 2 high angle symmetric scans are shown, where as reference bulk positions for Pd(200), FePd(200), FePd(002), V(200), and FeV(200) peaks are indicated as dotted lines, extracted from Refs. 1, 21, and 22. The angular region around $2\theta=24.4°$, where the FePd(100) peak is generally observed in chemically ordered structures, is not shown since no (001) was detected in our case, regardless of the alloy deposition temperature. This implies that no chemically ordered $L1_0$ phase is found in any sample. However, the strong evolution of the diffraction patterns as a function of deposition temperature indicates a temperature dependent structural modification at the atomic level in the layers. Regarding the FePd layer, FePd(200) diffraction peaks appear in all the samples, corresponding to the chemically disordered phase of FePd; a smooth evolution of the position of this peak is observed, indicating a slight and continuous change in the alloy lattice parameter. Consistently with the absence of FePd(001) reflections, the FePd(002) ones, characteristic also of the ordered $L1_0$ FePd phase and that should appear around $2\theta=49°$,[13] were not observed independently of the deposition temperature. Only two weak peaks around 50° appear for samples grown at 600 and 700 °C which could be due to a minoritary FePd ordered phase. Regarding the V buffer layer, the V(200) diffraction peak, whose bulk V position is $2\theta=61.3°$, is only detected at low deposition temperatures (RT and 100 and 200 °C), shifting to smaller scattering angles, with a small signal near bulk position for 300 °C, and disappearing in the sample grown at 400 °C. On the other hand, an additional peak appears in the sample grown at 200 °C in positions around $2\theta=65°$, the intensity increasing with the growth temperature and being maximum in the 600 °C sample. It has been already observed in Fe–V multilayers grown at high temperature[23–25] the thermal induced diffusion of V into the Fe layer and the alloying of Fe and V forming a body centered cubic (bcc) or a tetragonal σ phase depending on the stoichiometry and on the temperature.[26] The lattice parameter for this tetragonal σ phase is of 2.91 Å,[21] very close to the value extracted from the observed peaks. This is also very close to the Fe(200) reflection (Fe lattice parameter is 2.87 Å); therefore from these measurements it can be deduced that either the segregation of pure Fe regions or the formation of a FeV alloy

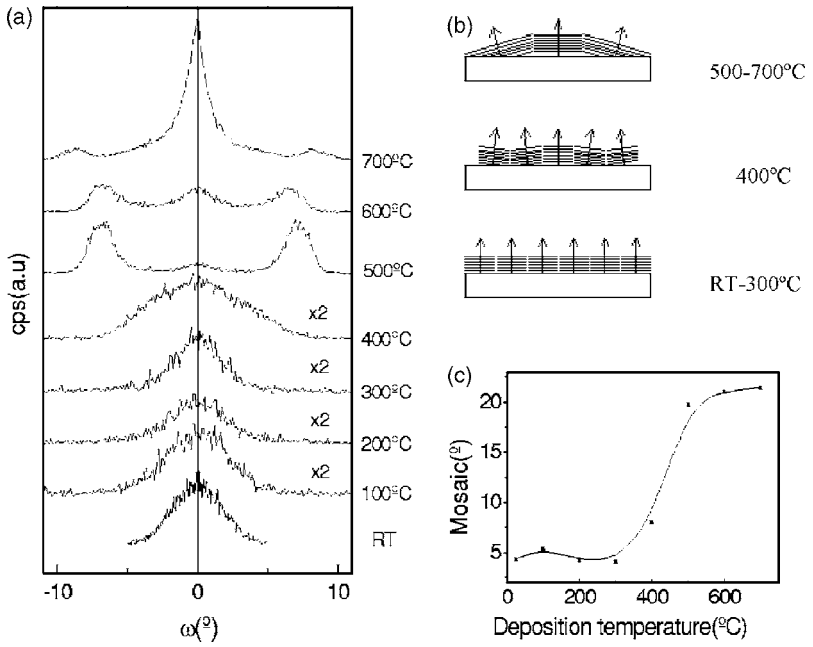

FIG. 3. (a) Rocking curves measured in the FePd(200) peaks, (b) sketch of the atomic plane evolution and (c) mosaic of the FePd films as a function of the deposition temperature.

occurs. In the sample grown at 700 °C no trace of V or other compounds is found; this disappearance has been previously observed in V layers grown at high temperature on MgO,[18] probably due to the V amorphization at these temperatures.

Additional structural information is presented in Fig. 3, where rocking curves measured around the FePd(200), V(200), and FeV(200) diffraction peaks are shown. The rocking curves corresponding to the V(200) diffraction peaks have an increasing width as the deposition temperature increases from RT to 300 °C (no V is found above 300 °C), being extracted a mosaic spread ranging from 2° to 10°. On the other hand rocking curves around the FeV(200) reflection exhibit a decreasing width with increasing temperature, ranging from 3° in the 200 °C sample to 1.5° at 600 °C; no trace of FeV is found at 700 °C. In the case of the FePd(200) peak [Fig. 3(a)], we observe distinctive regimes depending on the deposition temperature that clearly match those previously observed in AFM: from RT to 300 °C, where a flat morphology was obtained, the FePd mosaic remains constant with values around 4°. At 400 °C, where a transition from two-dimensional to three-dimensional morphology happened, a sudden increase of a factor of 2 in the mosaicity up to 8° is observed. Finally, above 400 °C the nature of the layer mosaic dispersion corresponds to that of a structure with a portion of crystallites aligned along the growth direction, as well as others misaligned with respect to it. In fact, for the sample grown at 500 °C the majority of crystallites are actually misaligned 7° with respect to the growth direction, according to the relative peak areas observed in the corresponding rocking curve, with a very small portion of the alloy planes still normally aligned. For the 600 °C sample the portion of misaligned crystallites (6.6° in this case) is reduced and that of the aligned ones increases, and finally for 700 °C most of the alloy particle crystalline planes (at this temperature the alloy is not continuous anymore) are aligned with the growth direction for this specific sample. In Fig. 3(b) a schematics of this interpretation about the mosaic structure evolution is depicted, together with a quantitative evolution of the mosaic dispersion as a function of the alloy deposition temperature in Fig. 3(c). There, the assigned values for the mosaic spread for 500–700 °C samples correspond to the separation of the measured peaks for the crystallites misaligned with respect to the growth direction.

The epitaxial relations between the substrate, buffer, and alloy layers were determined by measuring the asymmetric FePd(220), V(110), and MgO(110) reflections together with the V(200) and FePd(200) symmetric reflections, concluding the epitaxial relation: $[010](001)\mathrm{FePd}\|[-110](001)\mathrm{V}\|[010]\times(001)\mathrm{MgO}$, i.e., a 45° in-plane rotation of the V[100] direction with respect to the MgO and FePd ones. The out-of-plane (c) and in-plane (a) lattice parameters of the FePd, FeV, and V layers were also extracted from the position of the mentioned symmetric and asymmetric reflections, the corresponding results being presented in Fig. 4. The bulk lattice parameters are marked with a dashed line. A very small tetragonal distortion is observed in FePd at moderated deposition temperatures ($c/a=0.99$), much smaller than it would be expected for an ordered phase ($c/a=0.97$).[22] A tetragonal distortion is also observed in the FeV alloy phase, with a c/a ratio of 0.86.

In order to confirm the V diffusion in the FePd layer and to investigate the morphology and composition of the different layers, a combined TEM and EELS study was performed. This allows a simultaneous structural and chemical characterization with high spatial resolution. At low FePd deposition temperatures (100, 200, and 300 °C) very flat and crystalline alloy layers are observed, the epitaxial relationship with the substrate measured with XRD being confirmed. No interdiffusion of V or Pd appears in the FePd layers grown at low temperature as the EELS spectra demonstrate. The V(200) peak shift observed in the XRD between RT and 200 °C might be then due to epitaxial strain or very small interdiffusion, below the EELS detection limits. Figure 5(a) shows a TEM micrograph of the sample grown at 100 °C,

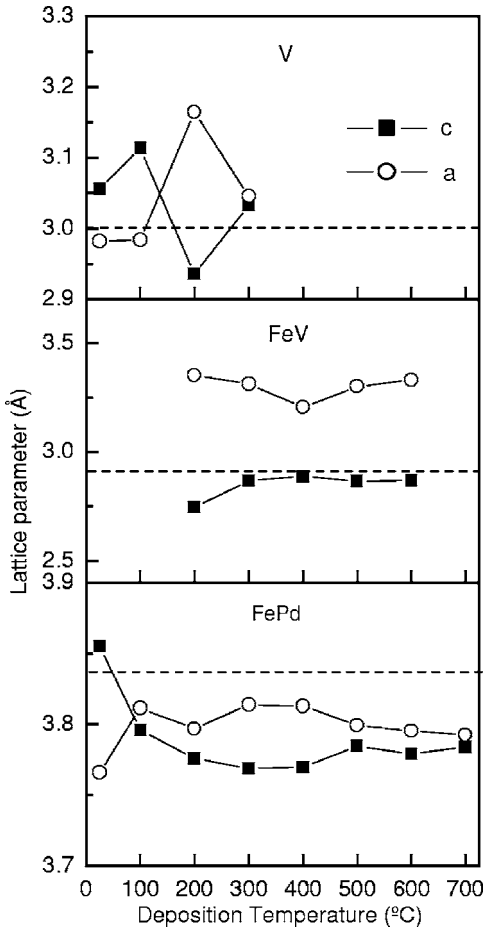

FIG. 4. Determined in-plane (a) and out-of-plane (c) lattice parameters of V, FeV, and FePd as a function of the deposition temperature. The bulk values are indicated in each case by a dashed line.

with a very well defined layered structure and clear interfaces: MgO, V, and FePd layers can be easily distinguished. Different EELS spectra were measured in the circled areas to investigate possible interdiffusion and the presence of V in the FePd layer. In Fig. 5(b) the spectra for the 100 °C sample measured in the marked areas are shown; the different peaks corresponding to the Pd $M_{4,5}$, V $L_{2,3}$, O K, and Fe $L_{2,3}$ transitions were investigated. However, no trace of the V $L_{2,3}$ peak appears in the FePd layer. In the sample grown at 400 °C, where a FeV alloy diffraction peak is already observed, the layered structure is not as well defined as for lower deposition temperatures [Fig. 5(c)]. Again, EELS spectra were taken in the circled regions [Fig. 5(d)] and this time V is found in the FePd layer, with a V content which is higher near the FePd–V interface, and that gradually reduces as we move farther away from it. This interdiffusion is also observed in the samples grown at higher temperature with increasing intensity. In the 700 °C sample there is no possibility to distinguish separate V and FePd layers [Fig. 5(e)] and the V concentration is found to be constant in all the FePd layers according to the relative V $L_{2,3}$ peak areas observed [Fig. 5(f)].

Complementary depth profiling XPS measurements were performed on samples grown at RT and high temperature (600 °C). The resulting concentrations of the different elements of interest (Fe, Pd, V, Mg, and O) as a function of thickness and for the two samples are presented in Fig. 6. As can be seen, for the sample grown at RT [Fig. 6(a)] the concentration of V exhibits a Gaussian distribution quenched in between the FePd film and the MgO substrate, indicating the presence of sharp interfaces and consequently the absence of V diffusion into the FePd thin film and in agreement with the conclusions extracted from the EELS measurements in the alloy grown at 100 °C. Note that the observation of sharp interfaces also indicates that no implantation phenomena are induced with Ar^+ ion with 1 keV kinetic energy. On the other hand, it can be clearly seen that for the sample grown at 600 °C [Fig. 6(b)] V is distributed in the whole FePd film and capping layer and that no sharp interfaces are observed. Such distribution of the V concentration as a function of thickness clearly indicates that, in contrast to the sample grown at RT, there is a strong diffusion of V into the FePd film. No clear changes in the chemical states of the V, Pd, and Fe elements could be observed on the core level spectra, probably due to the low concentration (always less than 5%) of the V and FeV alloys in the samples. As can be observed, the concentration ratio between Fe and Pd is close to 0.5 and almost constant in all the FePd layers and for both samples indicating the growth of a homogeneous and stoichiometric FePd compound.

IV. MAGNETIC AND MAGNETO-OPTICAL PROPERTIES

SQUID magnetometry has been used to obtain the saturation magnetization (M_s) of the samples. A value close to that of the stoichiometric phase at RT (1280 emu/cm^3) (Ref. 14) is found in the samples grown at lower temperatures (from RT to 300 °C), while a strong reduction is observed in the samples grown at higher temperature (400, 500, 600, and 700 °C) [Fig. 7(a)]. This change appears in the sample grown at 400 °C, in which the onset of V diffusion was observed by EELS; therefore the diffusion of V into the FePd layer and the appearance of FeV alloy with a lower average magnetization moment can explain the decrease of the saturation magnetization. It has been demonstrated that in Fe–V interfaces V couples antiferromagnetically with Fe, giving rise to a induced magnetization in V (magnetic moment per V atom ranging from $0.3\mu_B$ to $1.5\mu_B$), and a 20% decrease in the magnetic moment of Fe interface atoms.[27,28] This reduction has been observed as well in FeV alloys, measuring a magnetization of $0.99\mu_B$/at. for Fe (55% reduction) in equiatomic alloys[29] or even the total extinction for high concentrations of V. On the other hand in FePd the coupling is ferromagnetic and it has been calculated a magnetic moment of $3.04\mu_B$/at. for Fe exceeding the Fe value ($2.2\mu_B$/at.) and of $0.38\mu_B$/at. for Pd.[30]

Hysteresis loops for out-of-plane and in-plane fields have been measured by polar and transverse MOKEs; in Fig. 7(b) a complete characterization is shown: polar loops on the left column and the corresponding transverse loops on the right. In order to understand the magnetic behavior of the system we must keep in mind that two factors are competing: on one hand, the change in morphology from continuous

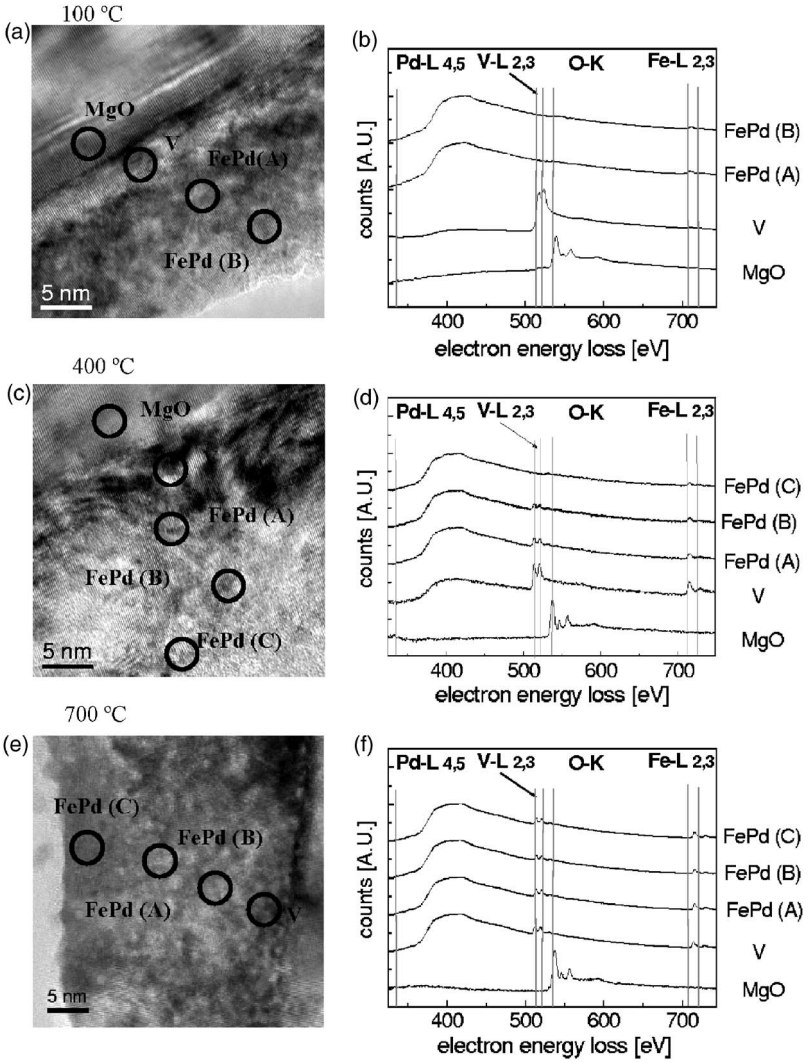

FIG. 5. (a), (c), and (e) TEM micrograph of the samples grown at 100, 400, and 700 °C, respectively. (b), (d), and (f) EELS spectra for the mentioned samples measured in the points marked in the images shown beside. The peaks Pd $M_{4,5}$, V $L_{2,3}$, O K, and Fe $L_{2,3}$ are studied. Note the absence of V in the FePd layer in the 100 °C sample, how V appears in different points of the FePd layer in the 400 °C sample, and the constant concentration of V along the FePd layer in the 700 °C sample.

films to three-dimensional islands as deposition temperature increases; and on the other hand, the FeV alloy formation between 400 and 700 °C as a consequence of the V interdiffusion. The samples grown at RT and 100 and 200 °C show a typical behavior of continuous thin films with in-plane magnetic anisotropy; they have a small in-plane coercive field and saturation field, and high out-of-plane saturation field.[31] They also exhibit a fourfold anisotropy, with easy [100] directions and hard [110] ones [shown in the transverse loops in Fig. 7(b)]. The sample grown at 300 °C is similar but the fourfold anisotropy has disappeared, probably due to the appearance of cracks in the layer that produces an additional configurational anisotropy which smears out the crystalline counterpart, as previously evidenced in Fe/MgO(001).[31] Again, the sample grown at 400 °C separates two different behavior regions in the magnetic response as it did in the structure and saturation magnetization. The in-plane coercive field increases from 6 to 150 Oe, due mainly to an increase in the nanoparticle height at that temperature (as observed by AFM and TEM) which leads to a smaller physical connection and therefore a weaker effective magnetic exchange between the nanoparticles; but also to the high dispersion of crystalline plane orientation (mosaic spread) observed in this sample. The increase of the out-of-plane coercive field and the big reduction of the out-of-plane saturation field point to the presence of perpendicular anisotropy, in spite of the absence of chemical order at this deposition temperature. Also in SQUID measurements where a higher field is applied and the sample gets saturated, an enormous increase of the in-plane saturation field (6 kOe) is observed in this sample, confirming the presence of a phase with perpendicular anisotropy. The samples grown at 500, 600, and 700 °C show a similar response as the one grown at 400 °C, with decreasing in-plane and out-of-plane coercivities. Also a decrease of the in-plane and an increase of the out-of-plane saturation fields are observed, indicative of a PMA phase. It is worth noticing that the PMA cannot be ascribed to the three-dimensional (3D) growth, since the nanoparticles exhibit a disklike shape with a maximum height/diameter ratio around 0.1 that is unlikely to promote perpendicular magnetization.

This clear correlation between reduced M_s (induced by a FeV alloy formation) and PMA, simultaneously observed in all the samples grown between 400 and 700 °C, indicates that the presence of the FeV alloy is responsible for the PMA. The magnetic anisotropy constant (K_u) calculated for the samples exhibiting PMA from the SQUID hysteresis loops measured along the in-plane direction reaches values

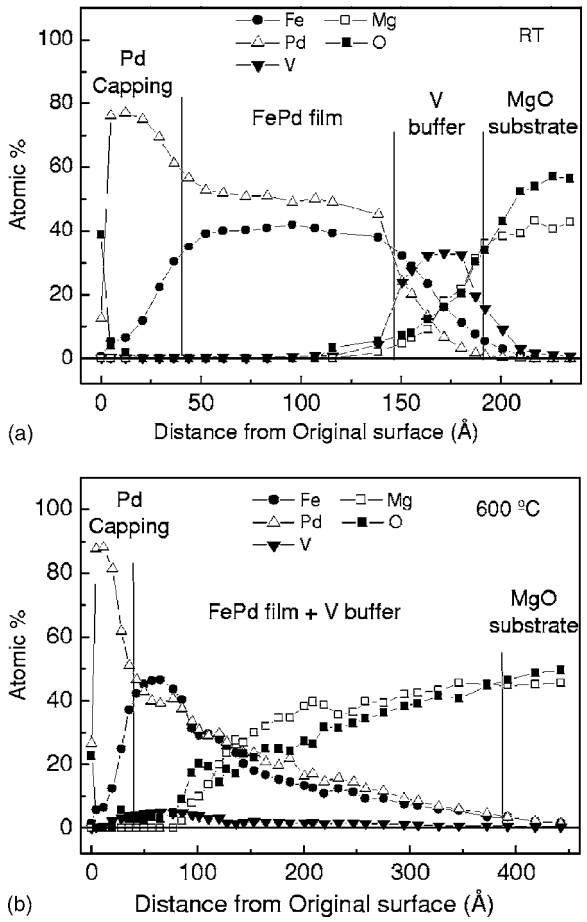

FIG. 6. Evolution of Pd, Fe, V, Mg, and O concentrations vs the distance from the surface, as detected by XPS for the samples grown at RT (a) and 600 °C (b).

of 5.2×10^4 J/m^3 for the 400 °C sample and 2.34×10^4 and 1.25×10^4 J/m^3 for the 500 and 700 °C samples, respectively. These values are quite below the one found in stoichiometric $L1_0$ FePd ordered alloy (9×10^5 J/m^3) but are quite high for a chemically disordered alloy.

MFM measurements confirm these findings. Figure 8 shows MFM images of three different samples at zero magnetic field. The images obtained with samples grown at high temperature exhibit alternate dark and bright regions, which is the distinctive feature of samples with perpendicular anisotropy:[32,33] these alternate regions correspond to up and down orientations of the magnetization. However, the sample grown at RT exhibits narrow lines that can be ascribed to magnetic domain walls,[34] meaning that elsewhere the magnetization lies mainly in plane of the film. It is worth noticing that low moment tips were needed in this MFM experiment to prevent the tip from dragging the domain walls.

To explore possible changes in electronic structure related with the FeV alloy formation, the MO spectral response of all the samples was investigated with polar Kerr spectroscopy in the photon energy range from 1.4 to 4.3 eV. In Fig. 9 the evolution of the Kerr rotation spectra as a function of deposition temperature is shown. While the samples grown at low temperature (RT and 100, 200, and 300 °C) show almost identical spectra, a strong change is observed in the sample grown at 400 °C, with an overall reduction of the

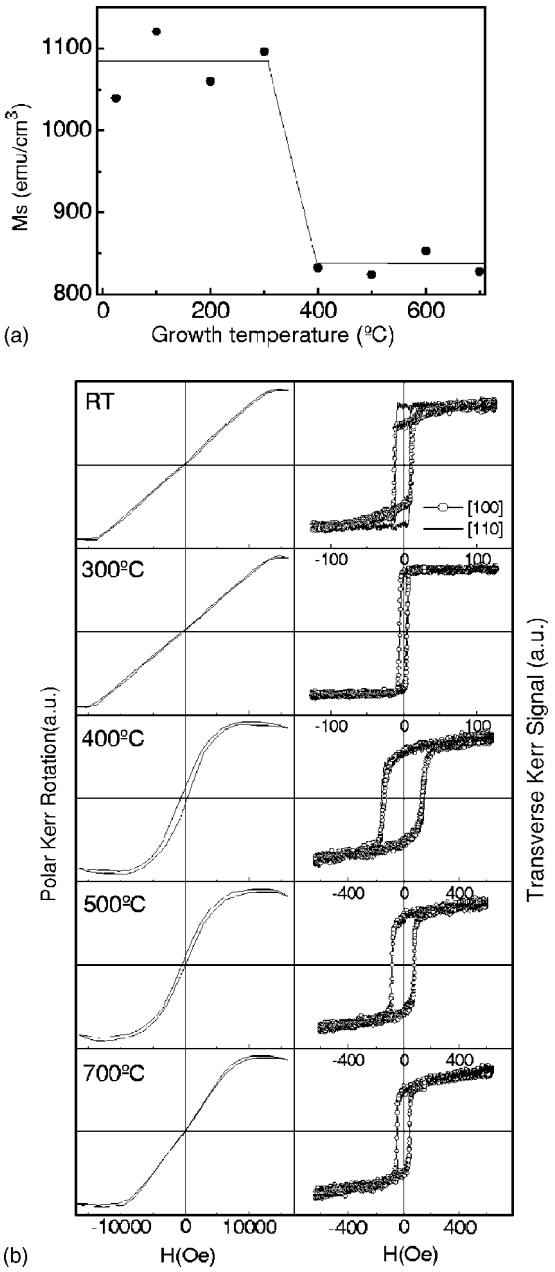

FIG. 7. (a) Saturation magnetization of the samples as a function of the deposition temperature measured with SQUID; the line is just a guide for the eyes. (b) Evolution of the polar (left) and transverse (right) Kerr loops with temperature. For the transverse loops, two curves are shown, one obtained for the [100] direction and the other for the [110] direction. Please note the different scales in the transverse loops.

Kerr rotation intensity and an even stronger reduction of the intensity of the 4 eV Kerr rotation peak in the sample grown at 700 °C. In FePd alloys this peak at 4 eV is related to the polarization of Pd induced by Fe,[35] the reduction of the intensity of this peak as we increase the growth temperature probably due to the presence of a FeV alloy. The V atoms will reduce the number of Pd atoms in contact with Fe and therefore their polarization, which will produce a reduction of the intensity of the Kerr rotation. The amount of FeV increases as deposition temperature increases due to the total diffusion of V in the FePd layers, as observed by EELS and XPS.

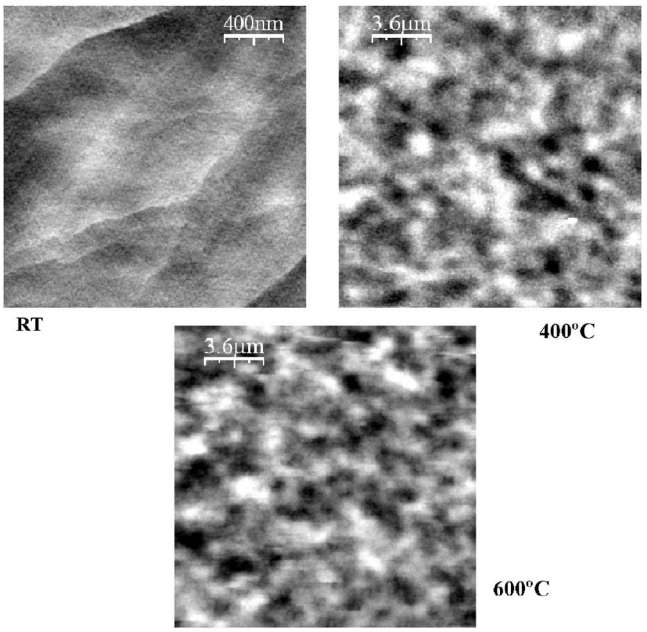

FIG. 8. MFM images of different samples. Sizes of 2×2 μm^2 for the RT sample and 18×18 μm^2 for the 400 and 600 °C samples.

V. CONCLUSIONS

We have studied the structure, morphology, composition, magnetism, and MO response of FePd films sputter deposited at different temperatures (from RT to 700 °C) on a monocrystalline V(001) buffer layer. Above 400 °C a strong V interdiffusion into the FePd layer and the formation of FeV alloy is accompanied by a two-dimensional to three-dimensional growth mode transition and an increase of the mosaic spread at these temperatures. A PMA phase is found in FeV–FePd films grown at temperatures above 400 °C in spite of the absence of long range chemical ordering, usually observed in FePd systems at high deposition temperature. We attribute the observed PMA to the V interdiffusion into the FePd layer and the formation of a FeV alloy. Although in this case PMA is obtained at similar temperatures as in regular FePd alloys, this approximation, i.e., FePd–FeV mixed systems, can open alternative ways to obtain high anisotropy systems at lower temperatures and with lower chemical order.

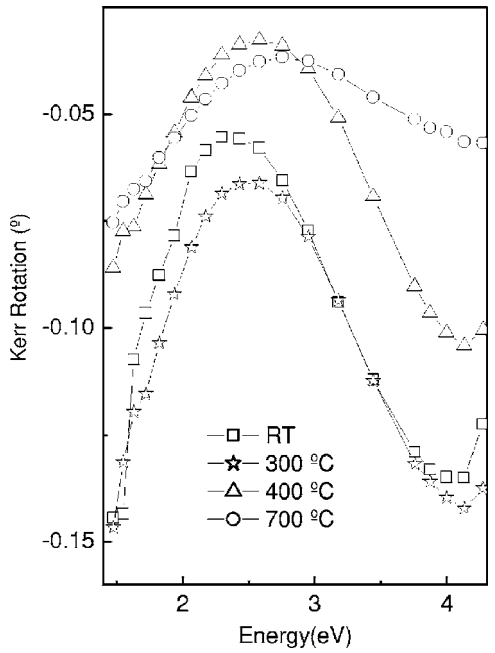

FIG. 9. Polar Kerr rotation spectra of the samples grown at different temperatures.

ACKNOWLEDGMENTS

This work was partially financed by the Spanish Commission of Science and Technology and Comunidad de Madrid. One of the authors (C.C.) acknowledges the Ministerio de Educación y Ciencia and FPI program for financial support. Two of the authors (J.M.G.-M. and Y.H.) acknowledge the Consejo Superior de Investigaciones Científicas (CSIC) and Ramón y Cajal program for financial support. The authors thank Dr. Elisa Román for the use of the XPS equipment and fruitful discussions.

[1] A. Cebollada, R. F. C. Farrow, and M. F. Toney, in *Magnetic Nanostructures*, edited by H. S. Nalwa (American Scientific Publishers, Los Angeles, 2002).
[2] D. Weller and A. Moser, IEEE Trans. Magn. **35**, 4423 (1999).
[3] S. Sun, C. B. Murray, D. Weller, L. Folks, and A. Moser, Science **287**, 1989 (2000).
[4] S. Sun, E. E. Fullerton, D. Weller, and C. B. Murray, IEEE Trans. Magn. **37**, 1239 (2001).
[5] P. Caro, A. Cebollada, F. Briones, and M. F. Toney, J. Cryst. Growth **187**, 426 (1998).
[6] T. Shima, K. Takanashi, Y. K. Takahashi, K. Hono, G. Q. Li, and S. Ishio, J. Magn. Magn. Mater. **266**, 171 (2003).
[7] T. Maeda, T. Kai, A. Kikitsu, T. Nagase, and J. Akiyama, Appl. Phys. Lett. **80**, 2147 (2002).
[8] Y. Endo, N. Kikuchi, O. Kitakami, and Y. Shimada, J. Appl. Phys. **89**, 7065 (2001).
[9] D. Ravelosona, C. Chappert, H. Bernas, D. Halley, Y. Samson, and A. Marty, J. Appl. Phys. **91**, 8082 (2002).
[10] T. Shima, T. Moriguchi, S. Mitani, and K. Takanashi, Appl. Phys. Lett. **80**, 288 (2002).
[11] T. Seki, T. Shima, K. Takanashi, Y. Takahashi, and E. Matsubara, Appl. Phys. Lett. **82**, 2461 (2003).
[12] Y. N. Hsu, S. Jeong, D. E. Laughlin, and D. N. Lambeth, J. Appl. Phys. **89**, 7068 (2001).
[13] P. Caro, A. Cebollada, D. Ravelosona, J. Tamayo, R. García, and F. Briones, Acta Mater. **46**, 2299 (1998).
[14] P. Caro, A. Cebollada, D. Ravelosona, F. Briones, D. García, M. Vázquez, and A. Hernando, J. Appl. Phys. **81**, 5050 (1997).
[15] M. F. Toney, W. Y. Lee, J. A. Hedstrom, and A. Kellock, J. Appl. Phys. **93**, 9902 (2003).
[16] D. Halley, B. Gilles, P. Bayle-Guillemaud, R. Arenal, A. Marty, G. Patrat, and Y. Samson, Phys. Rev. B **70**, 174437 (2004).
[17] Y. K. Takahashi, K. Hono, T. Shima, and K. Takanashi, J. Magn. Magn. Mater. **267**, 248 (2003).
[18] Y. Huttel, E. Navarro, and A. Cebollada, J. Cryst. Growth **273**, 474 (2005).
[19] M. S. Martín-González, Y. Huttel, A. Cebollada, G. Armelles, and F. Briones, Surf. Sci. **571**, 63 (2004).
[20] W. S. Kim, M. Aderholz, and W. Kleemann, Meas. Sci. Technol. **4**, 1275 (1993).
[21] M. Talanana, M. Benakki, F. Amalou, S. Bouarab, and C. Demangeat, Eur. Phys. J. B **22**, 497 (2001).
[22] W. Pearson, *Handbook of Lattice Spacings and Structures of Metals* (Pergamon, New York, 1958).
[23] A. Scherz, P. Poulopoulos, R. Nünthel, J. Lindner, H. Wende, F. Wilhelm, and K. Baberschke, Phys. Rev. B **68**, 140401 (2003).
[24] G. Andersson, E. Nordström, and R. Wäppling, Europhys. Lett. **60**, 731 (2002).
[25] J. F. M. Borges, J. B. M. da Cunha, and M. I. da Costa, Jr., J. Phys.:

Condens. Matter **15**, 1 (2003).
[26]J. M. Sanchez, M. C. Cadeville, V. Pierron-Bohnes, and G. Inden, Phys. Rev. B **54**, 8958 (1996).
[27]J. Izquierdo, A. Vega, O. Elmouhssine, H. Dreyssé, and C. Demangeat, Phys. Rev. B **59**, 14510 (1999).
[28]H. Fritzsche, Y. T. Liu, J. Hauschild, and H. Maletta, Phys. Rev. B **70**, 214406 (2004).
[29]J. C. Krause, J. Schaf, and M. I. da Costa, Jr., Phys. Rev. B **61**, 6196 (2000).
[30]D. García, R. Casero, M. Vázquez, and A. Hernando, Phys. Rev. B **63**, 104421 (2001).
[31]F. Cebollada, A. Hernando-Mañeru, A. Hernando, C. Martínez-Boubeta, A. Cebollada, and J. M. Gonzalez, Phys. Rev. B **66**, 174410 (2002).
[32]V. Gehanno, A. Marty, B. Gilles, and Y. Samson, Phys. Rev. B **55**, 12552 (1997).
[33]A. Asenjo, J. M. García, D. García, A. Hernando, M. Vázquez, P. A. Caro, D. Ravelosona, A. Cebollada, and F. Briones, J. Magn. Magn. Mater. **196–197**, 23 (1999).
[34]A. Wadas, M. Dreyer, M. Kleiber, and R. Wiesendanger, Appl. Phys. A: Mater. Sci. Process. **66**, 465 (1998).
[35]G. Armelles, D. Weller, B. Rellinghaus, P. Caro, A. Cebollada, and F. Briones, J. Appl. Phys. **82**, 4449 (1997).